EurJOC
European Journal of Organic Chemistry

Research Article
doi.org/10.1002/ejoc.202200718

Chemistry Europe
European Chemical Societies Publishing

www.eurjoc.org

Special Collection

Cyclic Triimidazoles as Stabilizers for Gene Promoter and Human Telomeric DNA G-Quadruplexes

Daniele Malpicci,[a, b] Stefano Andolina,[a] Stefano Di Ciolo,[a] Elena Lucenti,[b] Elena Cariati,[a, b] Simona Marzano,[c] Bruno Pagano,[c] Jussara Amato,[c] Antonio Randazzo,[c] and Clelia Giannini*[a]

Dedicated to Professor Cesare Gennari on the occasion of his 70th birthday.

The synthesis and characterization of a small series of cyclic triimidazole derivatives functionalized with methylated pyridine or guanidine moieties is reported. These compounds were tested for their ability to bind to G-quadruplexes from both telomeric and oncogene promoter sequences. Some of them exhibited high affinity and effective G-quadruplex-stabilizing properties. Overall, these compounds may represent useful leads for developing more potent and selective analogues.

Introduction

Triimidazo[1,2-*a*:1′,2′-*c*:1″,2″-*e*][1,3,5]triazine or cyclic triimidazole, hereafter **TT**, has recently revealed as an interesting photoluminescence compound characterized by aggregation-induced emissive (AIE) behavior, comprising, in particular, ultralong phosphorescence (RTUP) (lifetime up to 1 s) under ambient conditions associated with the presence of strong π-π stacking interactions in the crystalline structure.[1] Based on this, various **TT** derivatives have been developed and studied, so far, for their photophysical properties. The introduction of one or multiple halogen atoms on the **TT** scaffold results in a complex excitation dependent photoluminescent behavior including dual fluorescence, molecular and supramolecular phosphorescences, together with ultralong components.[2] Further substitution with chromophoric fragments such as 2-fluoropyridine,[3] 2-pyridine,[4] and pyrene (**TTPyr**)[5a,b] has enriched the photophysical behavior, preserving the solid state ultralong component. Moreover, based on the observation that triazinic functionalities are frequently used in the biological field[6] due to their ability to work as central scaffold for further modification or as mimetic of purine moieties,[7] **TTPyr** aggregates in water have been successfully tested for bioimaging applications, including potential cellular and bacterial imaging.[5a] In order to expand the scope and applicability of **TT**-based derivatives, here we report on the investigation of their potential use as DNA stabilizing agents. More precisely, this study was focused on G-quadruplex (G4), a non-canonical secondary structure of nucleic acids that self-folds within a DNA or RNA sequence containing contiguous guanine (G) repeats.[8,9] Formed by stacks of G-quartets, G4s are stabilized by the presence of monovalent cations, mainly K^+ and Na^+, which are highly abundant in the nucleus and cytoplasm, respectively. Interestingly, putative G4-forming sequences are distributed in genomic regions relevant for several pathologies, spanning from cancer to viral infections, where they can act as regulators of genetic information transfer. Multiple mapping and functional studies performed on human cells have revealed G4 involvement in the regulation of replication and transcription of oncogenes and other cancer-related genes, as well as DNA repair and maintenance of the stability of chromosome ends.[10,11] Therefore, targeting G-quadruplexes has become a novel promising antitumor strategy.[12–14] During the past two decades several efforts have been made in the search of small molecules able to recognize G4 structures. The common features of selective G4 ligands have been reported by several research groups.[15–17] Even though there are some notable exceptions,[18–19] in most cases these include extended planar aromatic systems that can stack on the external G-quartets, and the presence of positively charged tethered substituents for the interaction with the grooves and loops of the G4s and with the negatively charged phosphate DNA backbone. Based on the above characteristics, we envisaged that the **TT** scaffold shares certain structural features with known G4-binding small molecules, such as the potential for a flat conformation. Moreover, it can be mono-, di-, and tri-functionalized with different positively charged/(-able) groups capable of increasing ligand

[a] *Dr. D. Malpicci, S. Andolina, S. Di Ciolo, Prof. E. Cariati, Dr. C. Giannini*
Department of Chemistry
Università degli Studi di Milano and INSTM RU
Via Golgi 19, 20133, Milano, Italy
E-mail: clelia.giannini@unimi.it
[b] *Dr. D. Malpicci, Dr. E. Lucenti, Prof. E. Cariati*
Institute of Chemical Sciences and Technologies "Giulio Natta" (SCITEC) of CNR
Via Golgi 19, 20133, Milano, Italy
[c] *S. Marzano, Prof. B. Pagano, Prof. J. Amato, Prof. A. Randazzo*
Department of Pharmacy
University of Naples Federico II
Via D. Montesano 49, 80131, Napoli, Italy

Supporting information for this article is available on the WWW under https://doi.org/10.1002/ejoc.202200718

Part of the "Cesare Gennari's 70th Birthday" Special Collection.

Research Article
doi.org/10.1002/ejoc.202200718

binding to G4. Therefore, with the aim of assessing the ability to bind and stabilize biological relevant G-quadruplexes and to define the selectivity, we designed and prepared **TT** derivatives bearing polar and hydrophilic groups. In particular, we synthesized **TT** functionalized with one, two or three pyridine moieties attached to the central ring system via carbon 2 or carbon 4 (Scheme 1). The pyridinic fragments were further methylated with CH_3I obtaining positively charged water soluble derivatives with the charge at different distances from the central ring (Scheme 2). In parallel, a series of hydrophilic derivatives of **TT** has been prepared by reacting the corresponding mono-, di- and tri-formyl triimidazole with aminoguanidine (Scheme 3).[20–22] To our knowledge this is the first example of using the **TT** scaffold in the design of G4 ligands, thus opening new perspectives in this field.

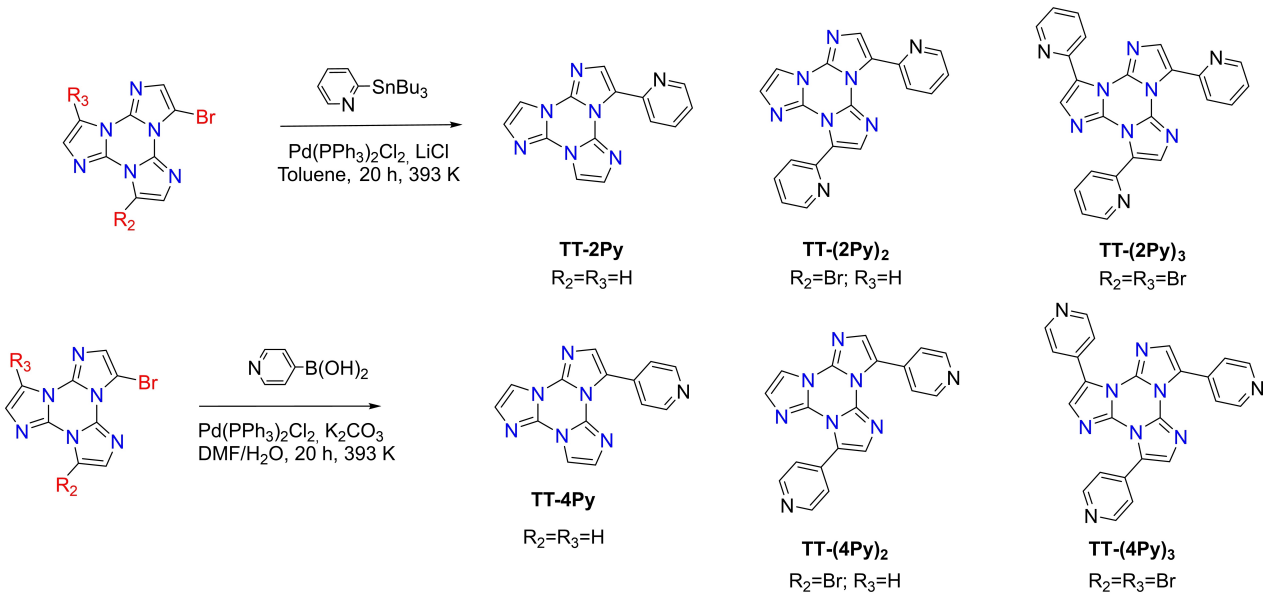

Scheme 1. Synthetic route to compounds **TT-2Py**, **TT-(2Py)$_2$**, **TT-(2Py)$_3$**, **TT-4Py**, **TT-(4Py)$_2$** and **TT-(4Py)$_3$**.

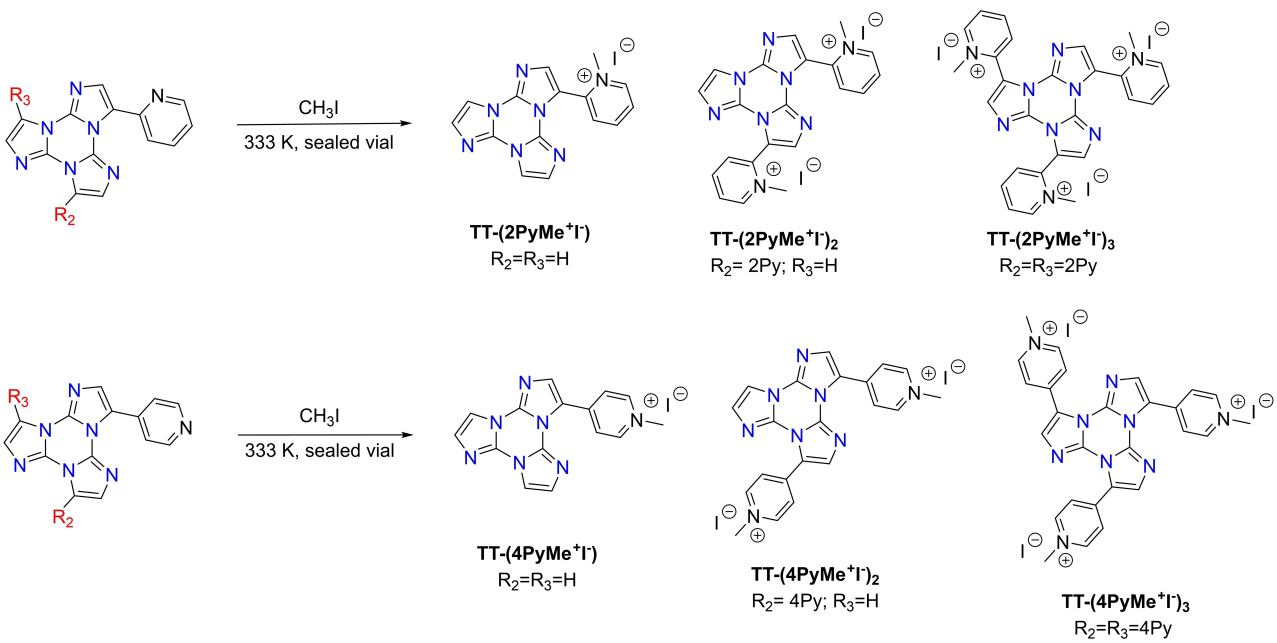

Scheme 2. Synthetic route to the methylated derivatives.

Research Article
doi.org/10.1002/ejoc.202200718

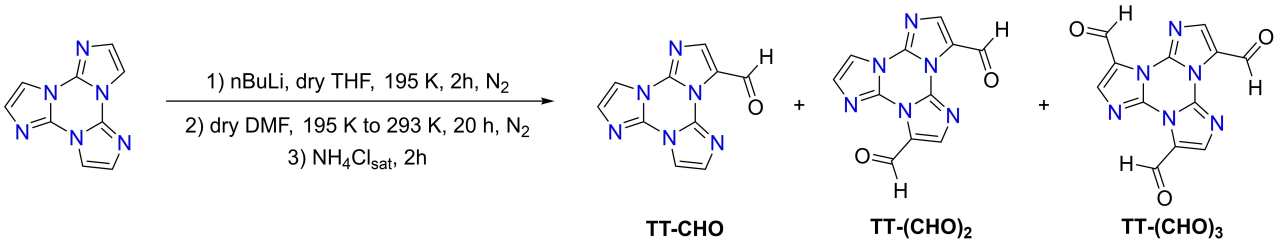

Scheme 3. Preparation of **TT-CHO**, **TT-(CHO)$_2$** and **TT-(CHO)$_3$**.

Results and Discussion

Synthesis of methylated pyridine TT derivatives

One, two or three pyridine moieties were bound to the **TT** scaffold starting from the corresponding **TT**-brominated derivatives. Subsequent methylation by reaction with CH_3I produced water soluble molecules with an aromatic, planar central core and 1, 2 or 3 more flexible and positively charged polar tails. Brominated derivatives, 3-bromotriimidazo[1,2-*a*:1′,2′-*c*:1″,2″-*e*][1,3,5]triazine, **TT-Br**, 3,7-dibromotriimidazo[1,2-*a*:1′,2′-*c*:1″,2″-*e*][1,3,5]triazine, **TT-Br$_2$** and 3,7,11-tribromotriimidazo[1,2-*a*:1′,2′-*c*:1″,2″-*e*][1,3,5]triazine, **TT-Br$_3$**, were prepared as previously reported[2a,b] and then reacted through Stille or Suzuki coupling to give the target compounds as shown in Scheme 1.

In particular, the 2-pyridine derivatives, **TT-2Py, TT-(2Py)$_2$** and **TT-(2Py)$_3$**, were prepared by Stille coupling of **TT-Br**, **TT-Br$_2$** and **TT-Br$_3$** with 2-(tributylstannyl)pyridine, then purified by standard chromatography techniques and characterized by NMR spectroscopy and mass spectrometry (see Experimental section). The 4-pyridine derivatives, namely **TT-4Py**, **TT-(4Py)$_2$** and **TT-(4Py)$_3$**, were prepared by Suzuki coupling between the proper brominated precursor and the corresponding, commercially available, 4-pyridinylboronic acid. The crude reaction products were purified by standard chromatographic techniques followed by precipitation to provide pure compounds.

In all obtained compounds, the nitrogen atoms of the pyridine rings were methylated by treatment with CH_3I to give the corresponding water-soluble derivatives (Scheme 2). It is interesting to stress the selective methylation of the pyridine fragments as supported by NMR data (see the Experimental). The nitrogen atoms of the triimidazole core require stronger methylating agents such as methyl trifluoromethanesulfonate.[23] The detailed description of the synthesis and characterization of all compounds is given in the Experimental Section.

Synthesis of guanyl hydrazone TT derivatives

The designed guanyl hydrazones **TT-Gn**, **TT-Gn$_2$** and **TT-Gn$_3$** (Scheme 4) were obtained by acid-catalyzed reaction of the corresponding aldehydes **TT-CHO**, **TT(CHO)$_2$** and **TT-(CHO)$_3$** with aminoguanidine hydrochloride (from now on **AG·HCl**) in high yield and purity, as hydrochloride salts, after workup and reverse-phase chromatography. To obtain the desired aldehydic precursors, **TT** was formylated *via* lithium salt intermediate (see Scheme 3). The reactive species were quenched with dry DMF and, after aqueous buffer work-up and chromatographic purification, afforded the corresponding aldehydes.

The formylation on **TT** was not specific and, depending on the number of equivalents of *n*BuLi, positions 3, 7 and 11 of the **TT** ring could be deprotonated and reacted with DMF providing a mixture of **TT-CHO**, **TT-(CHO)$_2$** and **TT-(CHO)$_3$**, according to NMR and mass spectrometry data.

An alternative approach for the introduction of the formyl group by means of the Vilsmeier-Haack reaction has been discarded due to the formation of several unidentified by-products and to lower yields of the desired derivative.

The three aldehydes were isolated with chromatographic techniques and completely characterized by means of NMR and mass spectrometry. In particular, the positions of the formyl

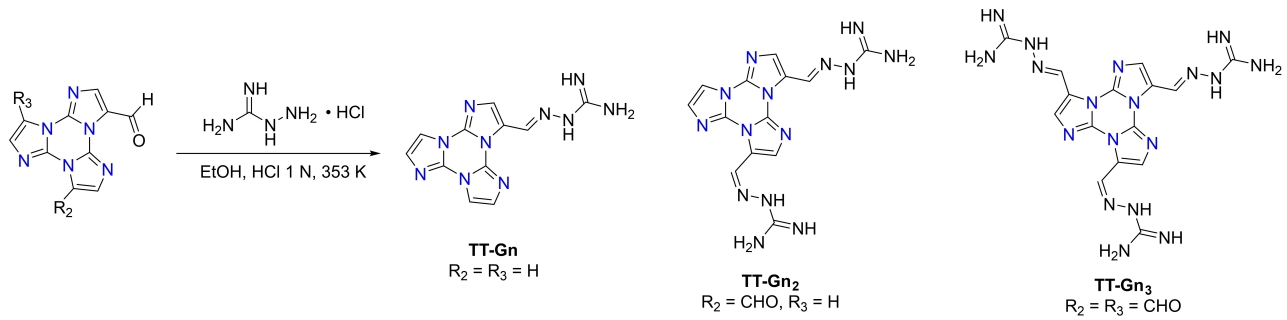

Scheme 4. Synthetic routes to guanyl hydrazone derivatives.

groups were determined using one- and two-dimensional NMR experiments (see Supporting Information). The purified aldehydes were then reacted with aminoguanidine hydrochloride to give the guanyl hydrazone derivatives **TT-Gn**, **TT-Gn$_2$** and **TT-Gn$_3$** as previously described (Scheme 4).

Biophysical evaluation of TT-derivatives' ability to bind to G-quadruplexes

To investigate the G4 binding properties of the synthesized molecules, *in vitro* biophysical studies were performed employing both telomeric and oncogene promoter G4-forming sequences. Three G4-forming sequences from the oncogene promoter regions of BCL-2 (*BCL2 G4*), c-KIT (*c-KIT2 G4*), and c-MYC (*c-MYC G4*), as well as a 26-mer truncation of the human telomeric DNA sequence (*Tel26 G4*), were used in these experiments. Changes in the topological aspects of each G4 DNA structure upon interaction with the **TT** derivatives here described were first investigated by circular dichroism (CD). CD spectra of *c-KIT2* and *c-MYC G4s* are characterized by a positive band at 262 nm and negative at 240 nm, confirming that they adopt a parallel-type G4 conformation[24,25] (hereafter *hybrid 1* form), while *BCL2 G4* exhibited two positive bands at around 260 and 290 nm, and a negative one at around 240 nm (Figure S49), according to the formation of a mixed parallel/antiparallel conformation.[26,27] As for the *Tel26 G4*, its CD spectrum shows two positive bands at around 290 and 270 nm, and a negative one at around 240 nm (Figure S49), which are characteristics of a [3 + 1] hybrid G4 (*hybrid 2* type-2) as major conformation.[28,29] Upon addition of each **TT**-derivative to the preformed G4 DNA, small changes in the intensities of CD signals were observed in the case of *c-KIT2*, *c-MYC* and *BCL2 G4s* suggesting that their overall topology is maintained in the presence of the compounds (Figure S50). Also, no substantial variations of the *Tel26 G4* spectra were observed upon addition of compounds containing the *o*-methylpyridinium fragment **TT-(2PyMe$^+$I$^-$)**, **TT-(2PyMe$^+$I$^-$)$_2$** and **TT-(2PyMe$^+$I$^-$)$_3$**. Conversely, the interaction of the *p*-methylpyridinium and guanyl hydrazone **TT** derivatives (**TT-(4PyMe$^+$I$^-$)**, **TT-(4PyMe$^+$I$^-$)$_2$**, **TT-(4PyMe$^+$I$^-$)$_3$** and **TT-Gn**, **TT-Gn$_2$**, **TT-Gn$_3$**) with *Tel26 G4* induced significant changes in its CD profile. Indeed, an increase in the intensity of the positive band at around 290 nm accompanied by the decrease or disappearance of that at 270 nm were observed (Figure 1), suggesting that such compounds induced a conformational conversion of *Tel26 G4* from hybrid-2 to hybrid-1 form.[30,31]

Next, the DNA stabilizing properties of all compounds were evaluated by CD-melting experiments, measuring the ligand-induced change in the melting temperature (ΔT_m) of each G4 (Figure S51). Results of these experiments, reported in Table 1 and summarized in Figure 2, indicated noteworthy G4-stabilizing effects for most of the investigated compounds even at low concentrations (2 molar equivalents of ligand). As expected for ligands having the same core but a different number of positive charges, the greater the charge number, the stronger the stabilizing effect on G4s. Indeed, the investigated compounds stabilized G4s according to the following order: compounds with three positively charged chains > two > one.

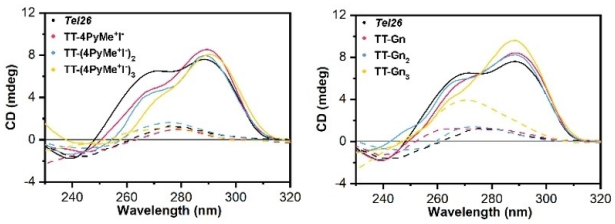

Figure 1. CD spectra at 20 and 100 °C (solid and dashed lines, respectively) recorded for *Tel26 G4* in 5 mM KH_2PO_4/K_2HPO_4 buffer (pH 7.0) containing 20 mM KCl in the absence and presence of 2 molar equiv. of compounds **TT-(4PyMe$^+$I$^-$)**, **TT-(4PyMe$^+$I$^-$)$_2$** and **TT-(4PyMe$^+$I$^-$)$_3$** and **TT-Gn**, **TT-Gn$_2$** and **TT-Gn$_3$**.

Table 1. Compound-induced thermal stabilization of the investigated G4s measured by CD melting experiments.

Compounds	ΔT_m [°C][a]			
	BCL2	*c-KIT2*	*c-MYC*	*Tel26*
TT-(2PyMe$^+$I$^-$)	-1.6 (±0.2)	1.9 (±0.2)	0.8 (±0.2)	0.9 (±0.2)
TT-(2PyMe$^+$I$^-$)$_2$	0.2 (±0.2)	1.0 (±0.2)	4.7 (±0.2)	2.1 (±0.2)
TT-(2PyMe$^+$I$^-$)$_3$	6.4 (±0.2)	4.3 (±0.2)	8.1 (±0.2)	5.0 (±0.2)
TT-(4PyMe$^+$I$^-$)	3.2 (±0.2)	7.0 (±0.2)	2.1 (±0.2)	6.6 (±0.2)
TT-(4PyMe$^+$I$^-$)$_2$	13.7 (±0.2)	15.3 (±0.2)	3.8 (±0.2)	16.6 (±0.2)
TT(4PyMe$^+$I$^-$)$_3$	> 30[b]	22.0 (±0.2)	2.1 (±0.2)	22.0 (±0.2)
TT-Gn	7.2 (±0.2)	11.0 (±0.2)	6.2 (±0.2)	2.3 (±0.2)
TT-Gn$_2$	> 30[b]	27.8 (±0.6)	10.8 (±0.2)	8.4 (±0.2)
TT-Gn$_3$	> 30[b]	27.7 (±0.2)	16.9 (±0.2)	11.7 (±0.2)

[a] ΔT_m is the difference between the T_m of DNA in the presence (2 molar equiv) and absence of compounds. T_m values in the absence of compounds are: *Tel26* = 44.6 (±0.1) °C; *BCL2* = 61.7 (±0.1) °C; *c-KIT2* = 59.0 (±0.1) °C and *c-MYC* = 67.9 (±0.1) °C. All experiments were performed in duplicate, and the reported values are the average of two measurements. [b] These compounds increased the thermal stability of the G4 to values at which it was not possible to accurately determine the T_m (see Supporting Information).

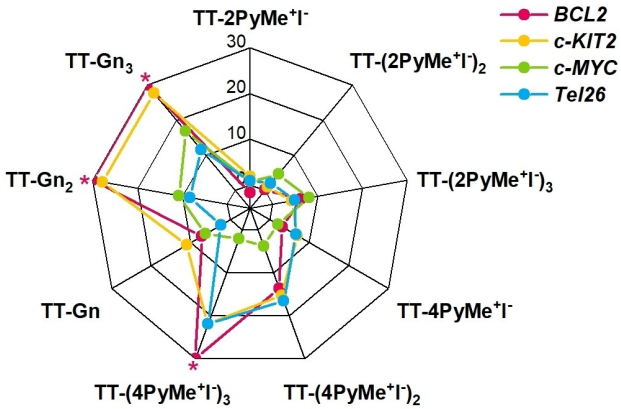

Figure 2. Spider chart showing the ligand-induced thermal stabilization of the G4s measured by CD melting experiments. ΔT_m values (Table 1) are plotted for each sequence. The asterisks indicate ΔT_m values that were not determined since these compounds increased the thermal stability of *BCL2 G4* to values at which it was not possible to determine the T_m.

Also, the position of the charge and the flexibility of the chain on which it is located, drastically affect the thermal stabilization properties of a ligand.[32] Here, the highest thermal stabilization effects were observed for the **TT** derivatives decorated with the guanyl hydrazone groups followed by the *p*-methylpyridinium ones, while the *o*-methylpyridinium substituents caused a drastic drop of the ligand-induced stabilization properties.

The investigated compounds did not exhibit ability to discriminate among the different G4 conformations (*i.e*, parallel, mixed and hybrid G4s), even if some of them (*i.e.* **TT-(4PyMe$^+$I$^-$)$_3$**, **TT-Gn$_2$** and **TT-Gn$_3$**) showed a certain preference for *BCL2* over the others, as indicated by the highest thermal stabilization effects observed in such cases (Figure 2).

To confirm the G4-stabilizing properties of the best compounds resulting from CD melting experiments (*i.e.*, **TT-(4PyMe$^+$I$^-$)$_3$**, **TT-Gn$_2$** and **TT-Gn$_3$**, Table 1) and to evaluate their ability to discriminate between G4 and duplex DNA, Förster resonance energy transfer (FRET) melting assays were also performed. In this assay, the FAM/TAMRA dual-labelled human telomeric G4 sequence (F21T) was used, which thanks to its low thermal stability allowed to estimate well the G4-stabilizing effects induced by ligands. Results showed in Table 2 confirmed the remarkable ability of **TT-(4PyMe$^+$I$^-$)$_3$**, **TT-Gn$_2$** and **TT-Gn$_3$** to stabilize the telomeric G4 and corroborated that the guanyl hydrazone moieties of **TT-Gn$_2$** and **TT-Gn$_3$** induced stronger stabilizing effects compared to the *p*-methylpyridinium ones of **TT-(4PyMe$^+$I$^-$)$_3$**, probably because of the higher flexibility of the formers, which could favor better interactions with the grooves/loops of G4s.

In addition, to assess ligands' selectivity for G4 over duplex DNA, FRET melting experiments were performed in the presence of a large excess of unlabeled competitor, here the double-stranded sequence (*ds26*). In these experiments, if the competitor has affinity for the ligand, it will sequester a significant fraction of it, which will be no longer available for fluorescent G4-forming oligonucleotide stabilization, leading to a decrease in T_m. The results of the experiments indicated a duplex concentration-dependent decrease of the G4/ligand thermal stabilities for **TT-(4PyMe$^+$I$^-$)$_3$**, **TT-Gn$_2$** and **TT-Gn$_3$** (Table 2 and Figure S52), suggesting the need of improving the selectivity of this class of molecules toward G4 structures.

Finally, to obtain quantitative data on the binding affinity of **TT-(4PyMe$^+$I$^-$)$_3$**, **TT-Gn$_2$** and **TT-Gn$_3$** for G4s and to estimate the degree of selectivity for G4 over duplex DNA, microscale thermophoresis (MST) experiments were carried out (Figure S53-S55).[33,34] This technique allows to evaluate equilibrium dissociation constants (K_d) by analyzing the ligand-induced changes in the thermophoretic behavior of a fluorescently labelled target molecule under microscopic temperature gradients. The results of MST experiments indicated that **TT-(4PyMe$^+$I$^-$)$_3$**, **TT-Gn$_2$** and **TT-Gn$_3$** were able to bind to *Tel26 G4* with equilibrium dissociation constants of 5.0 ($\pm$0.5), 3.0 ($\pm$2.0), and 3.2 ($\pm$0.7)$\times10^{-7}$ M, respectively. MST data suggested a slightly higher G4 binding affinity for **TT-Gn$_2$** and **TT-Gn$_3$** (with guanyl hydrazone substituents) rather than **TT-(4PyMe$^+$I$^-$)$_3$** (with *p*-methylpyridinium groups). Additional MST experiments were also recorded to evaluate the interaction of **TT-(4PyMe$^+$I$^-$)$_3$**, **TT-Gn$_2$** and **TT-Gn$_3$** with a hairpin-forming duplex model. K_d values of 9.5 ($\pm$5.0), 0.8 ($\pm$0.3), and 0.4 ($\pm$0.1) $\times10^{-6}$ M were obtained for **TT-(4PyMe$^+$I$^-$)$_3$**, **TT-Gn$_2$** and **TT-Gn$_3$**, respectively, suggesting a slight preference of **TT-(4PyMe$^+$I$^-$)$_3$** (with three 4-methylpyridinium substituents) for the telomeric G4 over duplex DNA, followed by **TT-Gn$_2$** (with two guanyl hydrazone substituents), while compound **TT-Gn$_3$** (with three guanyl hydrazone substituents) binds to the two DNA structures with the same affinity. Overall, these data suggest the possibility of addressing ligand selectivity by modulating the length, flexibility and number of the positively-charged side chains.

Table 2. Ligand-induced thermal stabilization of *F21T* G4 measured by FRET melting competition assays. ΔT_m values are the differences between the T_m of *F21T* in the presence (2 molar equiv. with respect to G4) and absence of the selected ligands, without or with large excesses of unlabeled duplex DNA (*ds26* at 15 and 50 molar equiv. with respect to G4).[a]

Compound	ΔT_m [°C]		
	F21T[a]	*F21T* + *ds26* (1:15)	*F21T* + *ds26* (1:50)
TT-(4PyMe$^+$I$^-$)$_3$	19.0	6.4	3.7
TT-Gn$_2$	22.4	7.1	2.3
TT-Gn$_3$	>30[b]	6.5	2.8

[a] T_m of *F21T* in the absence of ligands is 56.0 ($\pm$0.2) °C. Errors on ΔT_m values were $\pm$0.5 °C. All experiments were performed in duplicate, and reported values are the average of two measurements. [b] Because of the high ligand-induced G4 thermal stabilization, it was not possible to accurately determine the T_m value of the G4/ligand complex (see Supporting Information).

Conclusion

In summary, three families of **TT**-derivatives, namely the N-methylated 2-pyridine and 4-pyridine based and the guanidine-based ones, have been prepared and preliminary investigated for their binding affinities with G-quadruplexes. For each family, the stabilization increases on going from the mono-substituted to the three-substituted **TT**. Comparison between the two pyridine families reveals better affinity for the *para*-substituted one, highlighting the importance of the positive charge distance from the central **TT**-core. These results, not only open to the use of the aromatic **TT** scaffold as precursor of new G-quadruplex binders but also suggest the route for further chemical functionalization.

Experimental Section

General information. All reagents and model molecules were purchased from chemical suppliers and used without further purification unless otherwise stated. Triimidazo[1,2-*a*:1′,2′-*c*:1″,2″-*e*][1,3,5]triazine (**TT**),[35] **TT-Br**, **TT-Br$_2$**, **TT-Br$_3$**[2a,b] and **TT-2Py**[4] were prepared according to literature procedures. All solvents used for HPLC analysis were of LC–MS grade. Thin layer chromatography (TLC) was performed using Merck silica gel 60 F254 precoated plates. Column chromatography was carried out with Biotage™

apparatus equipped with silica gel Sfär Silica D Duo or Sfär C18 D-Duo 100 Å columns. ^{1}H and ^{13}C NMR spectra were recorded at 300 K on a Bruker AVANCE-400 instrument (400 MHz) equipped with a BBI 1H/Multinuclear Probe Chemical, shifts are reported in parts per million (ppm) and are referenced to the residual solvent peak (DMSO, ^{1}H: $\delta = 2.50$ ppm, ^{13}C: $\delta = 39.5$ ppm; CD_2Cl_2, ^{1}H: $\delta = 5.32$ ppm, ^{13}C: $\delta = 54.0$ ppm, DMF-d_7, ^{1}H: $\delta = 8.03$ ppm, ^{13}C: $\delta = 163.15$ ppm). Coupling constants (J) are given in hertz (Hz) and are quoted to the nearest 0.5 Hz. Peak multiplicities are described in the following way: s, singlet; d, doublet; t, triplet. Mass spectra were recorded on a Thermo Fisher LCQ Fleet Ion Trap Mass Spectrometer equipped with UltiMate™ 3000 high-performance liquid chromatography (HPLC) system. HRMS spectra were obtained using Synapt G2-Si QTof mass spectrometer (Waters) with Zspray™ ESI-probe for electrospray ionization (Waters). CPG supports, DNA phosphoramidites, all reagents for oligonucleotide synthesis and purification, and all other reagents and solvents were purchased from Merck KGaA (Darmstadt, Germany) and used without further purification. Dual-labeled FAM/TAMRA and Cy5.5-fluorescently labeled oligonucleotides were purchased from Biomers (Ulm, Germany).

*Synthesis of 1-methyl-2-(triimidazo[1,2-a:1′,2′-c:1″,2″-e][1,3,5]triazin-3-yl)pyridin-1-ium iodide (**TT-2PyMe$^+$I$^-$**).* **TT-(2PyMe$^+$I$^-$)** was prepared by methylation of **TT-2Py**. In a typical reaction, **TT-2Py** (100 mg; 0.36 mmol) and MeI (4 mL) were transferred inside a 20 mL closed vial equipped with a magnetic stirrer. The system was stirred at 60 °C for 48 h. The reaction mixture was then filtered on Büchner, washed with DCM to give **TT-(2PyMe$^+$I$^-$)** as a yellow solid (127 mg, 85% Yield). **NMR data (9.4 T, DMSO-d_6, 298 K, δ, ppm)** ^{1}H **NMR** δ 9.30 (d, $J = 6.2$, 1H), 8.76 (td, $J = 7.9$, 1.5 Hz, 1H), 8.40–8.23 (m, 2H), 8.15 (d, $J = 1.8$ Hz, 1H), 8.06 (d, $J = 1.7$ Hz, 1H), 7.77 (s, 1H), 7.41 (d, $J = 1.7$ Hz, 1H), 7.15 (d, $J = 1.7$ Hz, 1H), 4.21 (s, 3H); ^{13}C **NMR** δ 147.46, 145.61, 143.18, 138.02, 135.77, 135.19, 132.50, 132.20, 132.15, 128.96, 128.66, 128.46, 115.68, 112.13, 112.08, 111.87, 46.84. **HRMS** (ESI-positive ion mode): calcd for $C_{15}H_{12}N_7$ 290.1154 $[M]^+$, found 290.1152

*Synthesis of 3,7-di(pyridin-2-yl)triimidazo[1,2-a:1′,2′-c:1″,2″-e][1,3,5]triazine (**TT-(2Py)$_2$**).* **TT-(2Py)$_2$** was prepared by Stille coupling between **TT-Br$_2$** and 2-(tributylstannyl)pyridine. In a typical reaction, **TT-Br$_2$** (405 mg; 1.14 mmol), 2-(tributylstannyl)pyridine (1.00 mL, 3.37 mmol), LiCl (426 mg, 10.06 mmol), $Pd(PPh_3)_2Cl_2$ (24 mg, 0.03 mmol) and dry toluene (10 mL) were transferred inside a 100 mL Schlenk flask equipped with a magnetic stirrer. The mixture was deareated by means of three freeze-pump-thaw cycles. The system was heated under static nitrogen atmosphere at 130 °C for 72 h. The reaction was then cooled to room temperature, diluted with 50 mL of NaOH 1 M solution and extracted with DCM (3×30 mL). The organic phase was dried over Na_2SO_4, evaporated to dryness and the solid crude reaction mixture was further purified by automated flash chromatography on SiO_2 with DCM/MeOH as eluents to give the **TT-(2Py)$_2$** as a white solid (267 mg, 67% Yield). **NMR data (9.4 T, DMSO-d_6, 298 K, δ, ppm)** ^{1}H **NMR** δ 8.67 (m, 2H), 8.05 (m, 2H), 7.98 (d, $J = 1.7$ Hz, 1H), 7.91 (m, 2H), 7.55 (s, 1H), 7.42 (m, 3H), 7.22 (d, $J = 1.7$ Hz, 1H), ^{13}C **NMR** δ 148.8 (CH), 148.7 (CH), 147.3 (C), 147.2 (C), 135.6 (CH), 135.5(CH), 129.4(CH), 128.6 (CH), 128.0 (CH), 127.9 (C), 127.4 (C), 124.8 (CH), 124.7 (CH), 122.7 (CH), 122.6 (CH), 111.2 (CH). **MS** (ESI-positive ion mode): *m/z* 353.1$[M + H]^+$

*Synthesis of 1-methyl-2-(triimidazo[1,2-a:1′,2′-c:1″,2″-e][1,3,5]triazin-3-yl)pyridin-1-ium iodide (**TT-(2PyMe$^+$I$^-$)$_2$**).* **TT-(2PyMe$^+$I$^-$)$_2$** was prepared by methylation of **TT-(2Py)$_2$**. In a typical reaction, **TT-(2Py)$_2$** (55 mg; 0.36 mmol) and MeI (4 mL) were transferred inside a 20 mL closed vial equipped with a magnetic stirrer. The system was stirred at 60 °C for 240 h. The reaction mixture was then filtered on Büchner and washed with DCM to give **TT-(2PyMe$^+$I$^-$)$_2$** as a yellow solid (83 mg, 84% Yield). **NMR data (9.4 T, DMSO-d_6, 298 K, δ, ppm)** ^{1}H **NMR** δ 9.37 (d, $J = 6.2$ Hz, 1H), 9.32 (d, $J = 6.2$ Hz, 1H), 8.79 (dt, $J = 16.0$, 7.8 Hz, 2H), 8.38 (dt, $J = 17.6$, 7.6 Hz, 3H), 8.31–8.21 (m, 2H), 7.90 (s, 1H), 7.61 (s, 1H), 7.29 (d, $J = 1.7$ Hz, 1H), 4.24 (s, 3H), 4.14 (s, 3H). ^{13}C **NMR** δ 147.69, 145.86, 142.65, 142.57, 138.01, 137.35, 135.20, 132.87, 132.60, 132.44, 132.27, 129.23, 129.06, 128.99, 116.00, 115.73, 112.39, 47.01, 46.90. **HRMS** (ESI-positive ion mode): calcd for $C_{21}H_{18}N_8$ 191.0827 $[M]^{++}$, found 191.0825

*Synthesis of 3,7,11-tri(pyridin-2-yl)triimidazo[1,2-a:1′,2′-c:1″,2″-e][1,3,5]triazine (**TT-(2Py)$_3$**).* **TT-(2Py)$_3$** was prepared by Stille coupling between **TT-Br$_3$** and 2-(tributylstannyl)pyridine. In a typical reaction, **TT-Br$_3$** (200 mg; 0.46 mmol), 2-(tributylstannyl)pyridine (0.67 mL, 2.07 mmol), lithium chloride (292 mg, 6.90 mmol), $Pd(PPh_3)_2Cl_2$ (32 mg, 0.05 mmol) and dry toluene (10 mL) were transferred inside a dried 100 mL Schlenk flask equipped with a magnetic stirrer. The mixture was deareated by means of three freeze-pump-thaw cycles. The system was heated under static nitrogen atmosphere at 130 °C for 72 h. The reaction was then cooled to room temperature and evaporated to dryness. The crude was dissolved in DCM (30 mL) and NaOH 1 M (25 mL), extracted with DCM (3×30 mL). The organic phase was dried over Na_2SO_4, evaporated in vacuum and the solid crude reaction mixture was purified by chromatography on SiO_2 with DCM/MeOH 3.5% as eluents. Further precipitation from DCM/hexane gave the **TT-(2Py)$_3$** product as a white solid (41 mg, 21% Yield, Rf 0.17 in DCM/MeOH 5%). **NMR data (9.4 T, CD_2Cl_2, 298 K, δ, ppm)** ^{1}H **NMR** δ 8.70 (d, J = 4.8 Hz, 3H), 7.93 (d, J = 7.9 Hz, 3H), 7.84 (td, J = 7.8, 1.7 Hz, 3H), 7.38 (m, 6H). ^{13}C **NMR** δ 149.9 (CH), 148.2 (C), 137.2 (C), 136.4 (CH), 130.3 (CH), 129.0 (C), 125.7 (CH), 123.7 (CH). **MS** (ESI-positive ion mode): *m/z* 430,33 $[M + H]^+$

Synthesis of 2,2′,2″-(triimidazo[1,2-*a*:1′,2′-*c*:1″,2″-*e*][1,3,5]triazine-3,7,11-triyl)tris(1-methylpyridin-1-ium) iodide *(**TT-(2PyMe$^+$I$^-$)$_3$**).* **TT-(2PyMe$^+$I$^-$)$_3$** was prepared by methylation of **TT-(2Py)$_3$**. In a typical reaction, **TT-(2Py)$_3$** (45 mg; 0.10 mmol) and MeI (8 mL) were transferred inside a 20 mL closed vial equipped with a magnetic stirrer. The system was stirred at room temperature for 720 h. The reaction mixture was then filtered on Büchner and washed with DCM to give the **TT-(2PyMe$^+$I$^-$)$_3$** product as a yellow solid (71 mg, 80% Yield). **NMR data (9.4 T, DMSO-d_6, 298 K, δ, ppm)** ^{1}H **NMR** δ 9.38 (d, $J = 6.2$ Hz, 2H), 8.82 (t, $J = 7.9$ Hz, 2H), 8.42 (t, $J = 7.2$ Hz, 2H), 8.31 (d, $J = 7.9$ Hz, 2H), 7.74 (s, 2H), 4.23 (s, 9H). ^{13}C **NMR** δ 148.2 (CH), 146.2 (CH), 133.3 (CH), 132.6 (CH), 129.2 (CH), 46.9 (CH). **HRMS** (ESI-positive ion mode): calcd for $C_{27}H_{24}N_9$ 158.07127 $[M]^{+++}$, found 158.0718

*Synthesis of 3-(pyridin-4-yl)triimidazo[1,2-a:1′,2′-c:1″,2″-e][1,3,5]triazine (**TT-4Py**).* **TT-4Py** was prepared by Suzuki coupling between **TT-Br** and 4-pyridinylboronic acid. In a typical reaction, **TT-Br** (300 mg; 1.09 mmol), 4-pyridinylboronic acid (186 mg, 1.52 mmol), potassium carbonate (748 mg, 5.41 mmol), $Pd(PPh_3)_2Cl_2$ (76 mg, 0.11 mmol), water (3 mL) and DMF (8 mL) were transferred inside a 100 mL Schlenk flask equipped with a magnetic stirrer. The system was heated under static nitrogen atmosphere at 130 °C for 12 h. The reaction was then cooled to room temperature, evaporated to dryness and the crude purified using chromatography on SiO_2 with DCM/MeOH 3.5% as eluents to give the **TT-4Py** as a white solid. (119 mg, 40% yield, Rf 0.27 in DCM/MeOH 5%). **NMR data (9.4 T, DMSO-d_6, 298 K, δ, ppm)** ^{1}H **NMR** δ 8.65 (m, 2H), 8.00 (d, $J = 1.7$ Hz, 1H), 7.99 (d, $J = 1.7$ Hz, 1H), 8.82 (m, 2H), 7.60 (s, 1H), 7.32 (d, $J = 1.7$ Hz, 1H), 7.24 (d, $J = 1.7$ Hz, 1H), ^{13}C **NMR** δ 149.3 (CH), 137.8 (C), 135.98 (C), 135.78 (C), 135.68 (C), 129.7 (CH), 128.7 (CH), 128.0 (CH), 125.7 (C), 123.5 (CH), 111.9 (CH), 111.5(CH). **MS** (ESI-positive ion mode): *m/z*: 276.21 $[M + H]^+$

*Synthesis of 1-methyl-4-(triimidazo[1,2-a:1′,2′-c:1″,2″-e][1,3,5]triazin-4-yl)pyridin-1-ium iodide (**TT-4PyMe$^+$I$^-$**).* **TT-4PyMe$^+$I$^-$** was prepared by methylation of **TT-4Py**. In a typical reaction, **TT-4Py** (100 mg;

0.36 mmol) and MeI (4 mL) were transferred inside a 20 mL closed vial equipped with a magnetic stirrer. The system was heated at 60 °C for 24 h. The reaction mixture was then filtered on Büchner and washed with DCM to give **TT-4PyMe$^+$I$^-$** as a yellow solid (136 mg, 90% Yield). **NMR data (9.4 T, DMSO-d_6, 298 K, δ, ppm) ^{1}H NMR** δ 9.00 (d, J=8 Hz 2H), 8.65 (d, J=8 Hz 2H), 8.18 (s, 1H), 8.10 (dd, J=7.3, 1.7 Hz, 2H), 7.39 (d, J=1.7 Hz, 1H), 7.33 (d, J=1.7 Hz, 1H), 4.33 (s, 3H); **^{13}C NMR** δ 144.6, 142.6, 140.0, 135.8, 135.7, 135.5, 129.1, 127.8, 124.6, 123.4, 112.1, 111.9, 47.1. **HRMS** (ESI-positive ion mode): calcd for $C_{15}H_{12}N_7$ 290.1154 $[M]^+$, found 290.1153.

*Synthesis of 3,7-di(pyridin-2-yl)triimidazo[1,2-a:1′,2′-c:1″,2″-e][1,3,5]triazine (**TT-(4Py)$_2$**).* **TT-(4Py)$_2$** was prepared by Suzuki coupling between **TT-Br$_2$** and pyridin-4-ylboronic acid. In a typical reaction, **TT-Br$_2$** (250 mg; 0.70 mmol), pyridin-4-ylboronic acid (181 mg, 1.47 mmol), potassium carbonate (971 mg, 7.03 mmol), $Pd(PPh_3)_2Cl_2$ (49 mg, 0.07 mmol), dioxane (8 mL) and water (2 mL) were transferred inside a 100 mL Schlenk flask equipped with a magnetic stirrer. The system was heated under static nitrogen atmosphere at 130 °C for 24 h. The reaction mixture was then cooled to room temperature, filtered on Büchner and solvent evaporated under vacuum. Crude was further purified by automated flash chromatography on SiO_2 with DCM/ACN/MeOH as eluents to give the **TT-(4Py)$_2$** product as a white solid (190 mg, 77% Yield, Rf 0.37 in DCM/ACN 50%/MeOH 10%). **NMR data (9.4 T, DMSO-d_6, 298 K, δ, ppm) ^{1}H NMR** δ 8.68 (m, 4H), 8.05 (d, J=1.5 Hz, 1H), 7.79 (m, 4H), 7.62 (s, 1H), 7.42 (s, 1H), 7.28 (d, J=1.5 Hz, 1H). **^{13}C NMR** δ 149.2 (CH), 137.9, (C), 137.6(C), 135.6 (C), 135.5 (C), 130.0 (CH), 129.1 (CH), 128.3 (CH), 125.7 (C), 125.2 (C), 123.5 (CH), 123.4 (CH), 111.6 (CH). **MS** (ESI-positive ion mode): *m/z* 353.27 $[M+H]^+$

*Synthesis of 4,4′-(triimidazo[1,2-a:1′,2′-c:1″,2″-e][1,3,5]triazine-3,7-diyl)bis(1-methylpyridin-1-ium) iodide (**TT-(4PyMe$^+$I$^-$)$_2$**).* **TT-(4PyMe$^+$I$^-$)$_2$** was prepared by methylation of **TT-(4Py)$_2$**. In a typical reaction, **TT-(4Py)$_2$** (68 mg; 0.19 mmol) and MeI (2 mL) were transferred inside a 20 mL closed vial equipped with a magnetic stirrer. The system was stirred at room temperature for 60 h. The reaction mixture was then filtered on Büchner to give the **TT-(4PyMe$^+$I$^-$)$_2$** product as a yellow solid (105 mg, 86% Yield). **NMR data (9.4 T, DMSO-d_6, 298 K, δ, ppm) ^{1}H NMR** δ 9.04 (d, J=6.9 Hz, 4H), 8.60 (d, J=6.9 Hz, 4H), 8.26 (d, J=1.7 Hz, 1H), 8.23 (s, 1H), 8.12 (s, 1H), 7.42 (d, J=1.7 Hz, 1H), 4.36 (s, 6H).**^{13}C NMR** δ 144.83, 144.80, 142.35, 142.22, 140.03, 139.82, 136.11, 135.80, 134.44, 128.77, 125.17, 124.98, 123.63, 123.36, 112.48, 47.36, 47.33. **MS** (ESI-positive ion mode): *m/z* 191 $[M+H]^+$. **HRMS** (ESI-positive ion mode): calcd for $C_{21}H_{18}N_8$ 191.0827 $[M]^{++}$, found 191.0824.

*Synthesis of 3,7,11-tri(pyridin-4-yl)triimidazo[1,2-a:1′,2′-c:1″,2″-e][1,3,5]triazine (**TT-(4Py)$_3$**).* **TT-(4Py)$_3$** was prepared by Suzuki coupling between **TT-Br$_3$** and pyridin-4-ylboronic acid. In a typical reaction, **TT-Br$_3$** (250 mg; 0.57 mmol), pyridin-4-ylboronic acid (219 mg, 1.78 mmol), potassium carbonate (795 mg, 5.75 mmol), $Pd(PPh_3)_2Cl_2$ (40 mg, 0.06 mmol), dioxane (8 mL) and water (2 mL) were transferred inside a 100 mL Schlenk flask equipped with a magnetic stirrer. The system was heated under static nitrogen atmosphere at 130 °C for 24 h. The reaction mixture was then cooled to room temperature, filtered on Büchner and solvent evaporated under vacuum. The reaction crude was further purified by automated flash chromatography on SiO_2 with DCM/ACN/MeOH as eluents to give the **TT-(4Py)$_3$** product as a white solid (191 mg, 44% Yield, Rf 0.19 in DCM/ACN 50%/MeOH 10%). **NMR data (9.4 T, CH_2Cl_2-d_2, 298 K, δ, ppm) ^{1}H NMR** δ 8.71 (d, 6H), 7.67 (d, 6H), 7.30 (s, 3H). **^{13}C NMR** δ 150.11, 137.43, 135.93, 130.15, 127.11, 124.51. **MS** (ESI-positive ion mode): *m/z* 430.2 $[M+H]^+$

*Synthesis of 4,4′-(triimidazo[1,2-a:1′,2′-c:1″,2″-e][1,3,5]triazine-3,7-diyl)bis(1-methylpyridin-1-ium) iodide (**TT-(4PyMe$^+$I$^-$)$_3$**).* **TT-(4PyMe$^+$I$^-$)$_3$** was prepared by methylation of **TT-(4-Py)$_3$**. In a typical reaction, **TT-(4Py)$_3$** (203 mg; 0.47 mmol) and MeI (2 mL) were transferred inside a 20 mL closed vial equipped with a magnetic stirrer. The system was stirred at room temperature for 60 h. The reaction mixture was then filtered on Büchner to give the **TT-(4PyMe$^+$I$^-$)$_3$** product as a yellow solid (209 mg, 52% Yield). **NMR data (9.4 T, DMSO-d_6, 298 K, δ, ppm) ^{1}H NMR** δ 9.09 (m, 6H), 8.54 (m, 6H), 8.18 (s, 3H), 4.39 (s, 9H). **^{13}C NMR** δ 144.9, 142.0, 139.9, 135.1, 125.5, 123.7, 47.5, 40.1. **HRMS** (ESI-positive ion mode): calcd for $C_{27}H_{24}N_9$ 158.07127 $[M]^{+++}$, found 158.0718.

General Procedure for the Synthesis of the Aldehydes TT-CHO, TT-(CHO)$_2$ and TT-(CHO)$_3$. A *n*-BuLi 2.5 M hexane solution (*case a*: 1.5 eq. of *n*-BuLi, *case b*: 4.5 eq. of *n*-BuLi) was added dropwise under stirring to a solution of **TT** (500 mg, 2.5 mmol) in dry THF (30 mL) at −78 °C. The solution was stirred for 2 hour at −78 °C and then treated with dry DMF (*case a*: 240 mg, 3.75 mmol; *case b*: 720 mg, 11.2 mmol) and stirred overnight under static nitrogen up to room temperature (the colour of the solution changes to pale yellow). The solution was quenched with a saturated aqueous solution of NH_4Cl (5 mL). The THF was removed under reduced pressure, the crude material was taken up with water and extracted with AcOEt (3x60 mL). The organic phases were dried over Na_2SO_4, the solvent was removed under reduced pressure, and the crude material was purified by column chromatography using *n*-Hex/AcOEt (3:7) as eluent, affording: *case a*: 100 mg (17% Yield) of **TT-CHO** and 80 mg (13% Yield) of **TT-(CHO)$_2$**; *case b*: 50 mg (8% Yield) of **TT-CHO**; 45 mg (7% Yield) of **TT-(CHO)$_2$** and 95 mg (14% Yield) of **TT-(CHO)$_3$**.

*Triimidazo[1,2-a:1′,2′-c:1″,2″-e][1,3,5]triazine-3-carbaldehyde (**TT-CHO**).* **NMR data (7.05 T, DMSO-d_6, 298 K, δ, ppm) ^{1}H NMR** δ 10.76 (s, 1H), 8.12 (s, 1H), 8.11 (d, J=1.7 Hz, 1H), 8.09 (d, J=1.7 Hz, 1H)„ 7.43 (d, J=1.7 Hz, 1H), 7.38 (d, J=1.7 Hz, 1H) **^{13}C NMR** δ 180.2, 138.7, 135.9, 135.7, 135.0, 129.1, 128.9, 128.2, 112.2, 111.9. **HRMS** (ESI-positive ion mode): calcd for $C_{10}H_7N_6O$ 227.0681 $[M+H]^+$, found 227.0678.

*Triimidazo[1,2-a:1′,2′-c:1″,2″-e][1,3,5]triazine-3,7-dicarbaldehyde (**TT-CHO**)$_2$.* **NMR data (9.4 T, DMF-d_7, 298 K, δ, ppm) ^{1}H NMR** δ 10.92, (s, 1H), 10.85 (s, 1H), 8.28 (d, J= 1.7 Hz, 1H), 8.27, (s, 1H), 8.24 (s, 1H), 7.59 (d, J=1.7 Hz, 1H). **^{13}C NMR** δ 181.3, 181.1, 140.1, 1939.9, 137.4, 136.7, 135.9, 131.1, 130.2, 129.6, 113.5. **HRMS** (ESI-positive ion mode): calcd for $C_{11}H_7N_6O_2$ 255.0630 $[M+H]^+$, found 255.0631.

*Triimidazo[1,2-a:1′,2′-c:1″,2″-e][1,3,5]triazine-3,7,11-tricarbaldehyde (**TT-CHO**)$_3$.* **NMR data (9.4 T, DMSO-d_6, 298 K, δ, ppm) ^{1}H NMR** δ 10.77 (s, 3H), 8.37 (s, 3H). **^{13}C NMR** δ 179.9, 138.6, 136.0, 128.1. **HRMS** (ESI-positive ion mode): calcd for $C_{12}H_7N_6O_3$ 283.0580 $[M+H]^+$, found 283.0582.

General Procedure for the Synthesis of the Guanyl hydrazones TT-Gn, TT-Gn$_2$ and TT-Gn$_3$. The appropriate aldehyde (0.5 mmol) was dissolved in ethanol and reacted with one equivalent of aminoguanidine hydrochloride suspended in ethanol and treated with hydrochloridric acid in order to achieve a solution. The reaction mixture was refluxed for 3–5 h according to a TLC test. The reaction mixture was then cooled to room temperature, filtered on Büchner and solvent evaporated under vacuum. Crude was further purified by automated flash chromatography on C-18 column with a gradient of H_2O/ACN to give: **TT-Gn** (71% Yield), **TT-Gn$_2$** (80% Yield) or **TT-Gn$_3$** (76% Yield) based on the starting aldehyde.

*2-(triimidazo[1,2-a:1′,2′-c:1″,2″-e][1,3,5]triazin-3-ylmethylene)hydrazinecarboximidamide (**TT-Gn**).* **NMR data (9.4 T, DMSO-d_6, 298 K, δ, ppm) ^{1}H NMR** δ 12.16 (broad s, 1H), 9.16 (s, 1H), 8.05 (d, J=1.7 Hz, 1H), 8.01 (d, J=1.7 Hz, 1H), 7.95 (s, 1H), 7.75 (broad s), 7.37 (d, J=1.7 Hz, 1H), 7.33 (d, J=1.7 Hz, 1H) **^{13}C NMR** δ 155.1, 136.8, 136.0, 135.8, 135.5, 128.7, 128.3, 128.28, 123.2, 111.8, 111.6.

HRMS (ESI-positive ion mode): calcd for $C_{11}H_{11}N_{10}$ 283.1168 $[M+H]^+$, found 283.1167.

2,2′-(triimidazo[1,2-a:1′,2′-c:1″,2″-e][1,3,5]triazine-3,7-diylbis(methanylylidene))bis(hydrazinecarboximidamide) (***TT-Gn$_2$***). **NMR data (9.4 T, DMSO-d$_6$, 298 K, δ, ppm) ^{1}H NMR** δ 12.31 (broad s, 2H), 9.18 (s, 1H), 9.15 (s, 1H), 8.11 (d, J = 1.7 Hz, 1H), 8.03 (s, 1H), 8.01 (s, 1H), 7.82 (broad s), 7.42 (d, J = 1.7 Hz, 1H) **^{13}C NMR** δ 155.1, 137.0, 136.7, 135.8, 135.7, 135.6, 128.9, 128.7, 128.2, 123.4, 123.0, 111.8. **HRMS** (ESI-positive ion mode): calcd for $C_{13}H_{15}N_{14}$ 367.1604 $[M+H]^+$, found 367.1601.

2,2′,2″-(triimidazo[1,2-a:1′,2′-c:1″,2″-e][1,3,5]triazine-3,7,11-triyltris(methanylylidene))tris(hydrazinecarboximidamide) (***TT-Gn$_3$***). **NMR data (9.4 T, DMSO-d$_6$, 298 K, δ, ppm) ^{1}H NMR** δ 12.31 (broad s, 3H), 9.17 (s, 3H), 8.08 (s, 3H), 7.84 (broad s). **^{13}C NMR** δ 155.1, 136.7, 135.4, 128.5, 123.2. **HRMS** (ESI-positive ion mode): calcd for $C_{15}H_{19}N_{18}$ 451.2040 $[M+H]^+$, found 451.2037.

Oligonucleotide Synthesis and Sample Preparation

The following deoxyribonucleotide sequences: d(GGGCGCGGGAGGAATTGGGCGGG) (*BCL2*); d(CGGGCGGGCGCTAGGGAGGGT) (*c-KIT2*); d(TGAGGGTGGGTAGGGTGGGTAA) (*c-MYC*); d(TTAGGGTTAGGGTTAGGGTTAGGGTT) (*Tel26*); and d(CAATCGGATCGAATTCGATCCGATTG) (*ds$_{26}$*) were chemically synthesized at a 1-μmol scale on an ABI 394 DNA/RNA synthesizer (Applied Biosystem, CA, USA), by using the standard β-cyanoethyl phosphoramidite solid-phase chemistry, as described elsewhere.[36] After synthesis, oligonucleotides were detached from the support and deprotected by treating with an aqueous solution of concentrated ammonia at 55 °C, for 17 h. The filtrates and washings were combined and concentrated under reduced pressure, redissolved in water and purified by a high-performance liquid chromatography (HPLC) system equipped with a Nucleogel SAX column (Macherey-Nagel, Duren Germany, 1000-8/46), using a 30 min linear gradient from 100% buffer A to 100% buffer B at a flow rate of 1 mL/min (buffer A: 20 mM KH_2PO_4/K_2HPO_4 aqueous solution (pH 7.0) containing 20% (v/v) CH_3CN; buffer B: 1.0 M KCl, 20 mM KH_2PO_4/K_2HPO_4 aqueous solution (pH 7.0), containing 20% (v/v) CH_3CN). The purified fractions were then desalted using C-18 cartridges (Sep-pak). The purity of the isolated oligomers was proved to be higher than 98% by NMR. Oligonucleotide samples were prepared in a buffer solution consisting of 5 mM KH_2PO_4/K_2HPO_4 (pH 7.0) and 20 mM KCl (or LiCl in the case of *c-MYC*, because of its high thermal stability) and their concentration was verified by measuring the UV absorption at 90 °C, considering the appropriate molar extinction coefficient values ε (λ = 260 nm) calculated by the nearest neighbor mode.[37] To achieve the correct folding of the DNA sequences, oligonucleotide solutions were annealed by heating at 90 °C for 5 min followed by slow cooling to room temperature, and stored overnight at 4 °C.

Circular Dichroism (CD) Experiments

CD experiments were carried out on a Jasco J-815 spectropolarimeter equipped with a PTC-423S/15 Peltier temperature controller. Spectra were recorded at 20 and 100 °C in the wavelength range of 230 − 320 nm and averaged over three scans. A scan rate of 100 nm/min, with a 0.5 s response time and 1 nm bandwidth were used. The buffer baseline was subtracted from each spectrum. CD experiments were recorded both in the absence and presence of compounds (2 molar equiv) added to the folded nucleic acid structures (around 20 μM DNA). Ligand stock solutions were 10 mM in pure DMSO. CD spectra of DNA/ligand mixtures were recorded 10 min after ligand addition. CD melting experiments were carried out in the 20 − 100 °C temperature range at a 1 °C/min heating rate by following changes of the CD signal at the wavelengths of the maximum CD intensity for each DNA (*i.e.*, 264 nm for *c-KIT2* and *c-MYC* G4s, 266 nm for *BCL2* G4, and 290 nm for *Tel26* G4). The melting temperatures (T_m) were determined from a curve fit using OriginPro© 2021 software (OriginLab Corp., MA, USA). ΔT_m values were determined as the difference in the T_m values of G4s in the presence and absence of the compounds. Normalization of melting curves between 0 and 1 was performed to better compare the results. In some cases, due to the exceptional ligand-induced G4 thermal stabilization (the melting process was not completed even at 100 °C), the relative melting curves were normalized by dividing only for the maximum.

FRET Melting Experiments

Measurements were carried out on a Jasco FP-8300 spectrofluorometer equipped with a Peltier temperature controller system (PCT-818) using the dual-labeled telomeric G4-forming sequence FAM-[d(GGGTTAGGGTTAGGGTTAGGG)]-TAMRA (*F21T*) and the double-stranded unlabeled DNA competitor, *ds$_{26}$*. *F21T* and *ds26* oligonucleotides were dissolved in 5 mM KH_2PO_4/K_2HPO_4 (pH 7.0) buffer containing 20 mM KCl at 1 μM and 1 mM single strand concentrations, respectively. Both oligonucleotide solutions were annealed by heating to 90 °C for 5 min, followed by slow cooling to room temperature overnight and storage at 4 °C for 24 h before data acquisition. Experiments were performed in sealed quartz cuvettes with a path length of 1 cm by using 0.2 μM of pre-folded *F21T* target, in the absence and presence of the ligand at 0.4 μM, and the duplex competitor (*ds$_{26}$*) at 3 and 10 μM final concentrations. In addition, a blank with no compound or competitor was also performed. Fluorescence spectra were acquired before and after the melting assay (15 and 90 °C, respectively). The dual-labeled oligonucleotide was excited at 492 nm, and emission spectra were recorded between 500 and 650 nm using a 100 nm/s scan speed. Excitation and emission slit widths were both set to 5 nm. FRET melting experiments were performed by monitoring the emission of FAM at 520 nm (upon excitation at 492 nm), using a heating gradient of 0.2 °C/min over the range 15–90 °C. The emission of FAM was normalized between 0 and 1. The final analysis of the data was carried out using OriginPro© 2021 software.

Microscale Thermophoresis (MST) Experiments

MST measurements were performed on a Monolith NT.115 (Nanotemper Technologies, Munich, Germany). Cy5.5-*Tel26* (Cy5.5-[d-(TTAGGGTTAGGGTTAGGGTTAGGGTT)]) and Cy5.5-*Hairpin-duplex* (Cy5.5-[d(CGCGAATTCGCGTTTCGCGAATTCGCG)]) were prepared at 1 μM single strand concentration in 5 mM KH_2PO_4/K_2HPO_4 buffer (pH 7.0) containing 20 mM KCl. Both oligonucleotides were annealed before use as described above. For the MST experiments, the concentration of the labeled oligonucleotides was kept constant at 50 nM, while a serial dilution of the ligand (1 : 2 from a solution 200, 15.0 or 2.4 μM of **TT-(4PyMe$^+$I$^-$)$_3$**, **TT-Gn$_2$** and **TT-Gn$_3$**, respectively) was prepared in the same buffer used for DNAs supplemented with 0.1% Tween and 10% DMSO. These solutions were then mixed with a volume ratio of 1 : 1, incubated for 15 min, and loaded into standard capillaries (NanoTemper Technologies, Munich, Germany). Measurements were performed at 20 °C using autotune LED power and medium MST power. MST data analysis was performed by employing the MO.Affinity Analysis software (v2.3) provided with the instrument.

Acknowledgements

C.G. and E.C. thanks Università degli Studi di Milano (Piano di Sostegno alla Ricerca Linea 2, Azione A – Project PSR2020_DIP_005_PI_ACOL) for financial support. The authors thank Marco Pappini and Milda Stuknyte for performing HR-MS spectra at the Mass Spectrometry facility of the Unitech COSPECT at the University of Milan. Open Access funding provided by Università degli Studi di Milano within the CRUI-CARE Agreement.

Conflict of Interest

The authors declare no conflict of interest.

Data Availability Statement

Data sharing is not applicable to this article as no new data were created or analyzed in this study.

Keywords: Aminoguanidine · Cyclic triimidazole · G-quadruplex · Ligand design · N-methylated pyridine

[1] E. Lucenti, A. Forni, C. Botta, L. Carlucci, C. Giannini, D. Marinotto, A. Previtali, S. Righetto, E. Cariati, *J. Phys. Chem. Lett.* **2017**, *8(8)*, 1894–1898.
[2] a) E. Lucenti, A. Forni, C. Botta, L. Carlucci, C. Giannini, D. Marinotto, A. Pavanello, A. Previtali, S. Righetto, E. Cariati, *Angew. Chem. Int. Ed.* **2017**, *56*, 16302–16307; b) E. Lucenti, A. Forni, C. Botta, L. Carlucci, A. Colombo, C. Giannini, D. Marinotto, A. Previtali, S. Righetto, E. Cariati, *ChemPhotoChem* **2018**, *2(9)*, 801–805; c) S. Di Micco, C. Giannini, A. Previtali, E. Lucenti, G. Bifulco, *Magn. Reson. Chem.* **2019**, *57(2–3)*, 82–92; d) E. Lucenti, A. Forni, C. Botta, C. Giannini, D. Malpicci, D. Marinotto, A. Previtali, S. Righetto, E. Cariati, *Chem. Eur. J.* **2019**, *25(10)*, 2452–2456; e) C. Giannini, A. Forni, D. Malpicci, E. Lucenti, D. Marinotto, A. Previtali, L. Carlucci, E. Cariati, *Eur. J. Org. Chem.* **2021**, *2021*, 2041–2049.
[3] A. Previtali, E. Lucenti, A. Forni, L. Mauri, C. Botta, C. Giannini, D. Malpicci, D. Marinotto, S. Righetto, E. Cariati, *Molecules* **2019**, *24*, 2552.
[4] E. Cariati, E. Lucenti, A. Forni, A. Previtali, D. Marinotto, D. Malpicci, S. Righetto, C. Giannini, T. Virgili, P. Kabacinski, L. Ganzer, U. Giovanella, C. Botta, *Chem. Sci.* **2020**, *11*, 7599–7608.
[5] a) A. Previtali, W. He, A. Forni, D. Malpicci, E. Lucenti, D. Marinotto, L. Carlucci, P. Mercandelli, M. A. Ortenzi, G. Terraneo, C. Botta, R. T. K. Kwok, J. W. Y. Lam, B. Z. Tang, E. Cariati, *Chem. Eur. J.* **2021**, *27(67)*, 16690–16700; b) D. Malpicci, C. Giannini, E. Lucenti, A. Forni, D. Marinotto, E. Cariati, *Photochemistry* **2021**, *1*, 477–487.
[6] L. Wackett, M. Sadowsky, B. Martinez, N. Shapir, *Appl. Microbiol. Biotechnol.* **2002**, *58*, 39–45.
[7] F. P. L. Lim, A. V. Dolzhenko, *Eur. J. Med. Chem.* **2014**, *85*, 371–390.
[8] M. L. Bochman, K. Paeschke, V. A. Zakian, *Nat. Rev. Genet.* **2012**, *13*, 770–780.
[9] S. Marzano, B. Pagano, N. Iaccarino, A. Di Porzio, S. De Tito, E. Vertecchi, E. Salvati, A. Randazzo, J. Amato, *Int. J. Mol. Sci.* **2021**, *22*, 10315.
[10] R. Hänsel-Hertsch, J. Spiegel, G. Marsico, D. Tannahill, S. Balasubramanian, *Nat. Protoc.* **2018**, *13*, 551–564.
[11] P. Zizza, C. Cingolani, S. Artuso, E. Salvati, A. Rizzo, C. D'Angelo, M. Porru, B. Pagano, J. Amato, A. Randazzo, E. Novellino, A. Stoppacciaro, E. Gilson, G. Stassi, C. Leonetti, A. Biroccio, *Nucleic Acids Res.* **2016**, *44*, 1579–1590.
[12] S. Balasubramanian, L. H. Hurley, S. Neidle, *Nat. Rev. Drug Discovery* **2011**, *10*, 261–275.
[13] N. Kosiol, S. Juranek, P. Brossart, A. Heine, K. Paeschke, *Mol. Cancer* **2021**, *20*, 1–18.
[14] I. Alessandrini, M. Recagni, N. Zaffaroni, M. Folini, *Int. J. Mol. Sci.* **2021**, *22*, 5947.
[15] a) D. Monchaud, M.-P. Teulade-Fichou, *Org. Biomol. Chem.* **2008**, *6*, 627–636; b) A. R. Duarte, E. Cadoni, A. S. Ressurreicao, R. Moreira, A. Paulo, *ChemMedChem* **2018**, *13*, 869–893.
[16] T. Santos, G. F. Salgado, E. J. Cabrita, C. Cruz, *Pharmaceuticals* **2021**, *14*, 769.
[17] D. Musumeci, J. Amato, P. Zizza, C. Platella, S. Cosconati, C. Cingolani, A. Biroccio, E. Novellino, A. Randazzo, C. Giancola, B. Pagano, D. Montesarchio, *Biochim. Biophys. Acta Gen. Subj.* **2017**, *1861*.
[18] B. Brassart, D. Gomez, A. De Cian, R. Paterski, A. Montagnac, K. H. Qui, N. Temime-Smaali, C. Trentesaux, J. L. Mergny, F. Gueritte, J. F. Riou, *Mol. Pharmacol.* **2007**, *72(3)*, 631–640.
[19] H. Tateishi-Karimata, N. Sugimoto, *Chem. Commun.* **2020**, *56*, 2379–2390.
[20] S. Sparapani, S. Bellini, M. Gunaratnam, S. M Haider, A. Andreani, M. Rambaldi, A. Locatelli, R. Morigi, M. Granaiola, L. Varoli, S. Burnelli, A. Leoni, S. Neidle, *Chem. Commun.* **2010**, *46*, 5680–5682.
[21] J. Amato, G. Miglietta, R. Morigi, N. Iaccarino, A. Locatelli, A. Leoni, E. Novellino, B. Pagano, G. Capranico, A. Randazzo, *J. Med. Chem.* **2020**, *63*, 3090–3103.
[22] J. Amato, R. Morigi, B. Pagano, A. Pagano, S. Ohnmacht, A. De Magis, Y.-P. Tiang, G. Capranico, A. Locatelli, A. Graziadio, A. Leoni, M. Rambaldi, E. Novellino, S. Neidle, A. Randazzo, *J. Med. Chem.* **2016**, *59*.
[23] M. Magni, E. Lucenti, A. Previtali, P. R. Mussini, E. Cariati, *Electrochim. Acta* **2019**, *317*, 272–280.
[24] S.-T. D. Hsu, P. Varnai, A. Bugaut, A. P. Reszka, S. Neidle, S. Balasubramanian, *J. Am. Chem. Soc.* **2009**, *131*, 13399–13409.
[25] A. Ambrus, D. Chen, J. Dai, R. A. Jones, D. Yang, *Biochemistry* **2005**, 44, 2048–2058.
[26] J. Dai, D. Chen, R. A. Jones, L. H. Hurley, D. Yang, *Nucleic Acids Res.* **2006**, *34*, 5133–5144.
[27] J. Amato, A. Pagano, D. Capasso, S. Di Gaetano, M. Giustiniano, E. Novellino, A. Randazzo, B. Pagano, *ChemMedChem* **2018**, *13*, 406–410.
[28] A. T. Phan, V. Kuryavyi, K. N. Luu, D. J. Patel, *Nucleic Acids Res.* **2007**, *35*, 6517–6525.
[29] J. Dai, M. Carver, D. Yang, *Biochimie* **2008**, *90*, 1172–1183.
[30] A. Ambrus, D. Chen, J. Dai, T. Bialis, R. A. Jones, D. Yang, *Nucleic Acids Res.* **2006**, *34*, 2723–2735.
[31] J. Dai, M. Carver, C. Punchihewa, R. A. Jones, D. Yang, *Nucleic Acids Res.* **2007**, *35*, 4927–4940.
[32] A. Di Porzio, U. Galli, J. Amato, P. Zizza, S. Iachettini, N. Iaccarino, S. Marzano, F. Santoro, D. Brancaccio, A. Carotenuto, S. De Tito, A. Biroccio, B. Pagano, G. C. Tron, A. Randazzo, *Int. J. Mol. Sci.* **2021**, *22*, 11959.
[33] J. Amato, C. Platella, S. Iachettini, P. Zizza, D. Musumeci, S. Cosconati, A. Pagano, E. Novellino, A. Biroccio, A. Randazzo, B. Pagano, D. Montesarchio, *Eur. J. Med. Chem.* **2019**, *163*, 295–306.
[34] J. Amato, T. W. Madanayake, N. Iaccarino, E. Novellino, A. Randazzo, L. H. Hurley, B. Pagano, *Chem. Commun.* **2018**, *54*, 9442–9445.
[35] D. M. Schubert, D. T. Natan, D. C. Wilson, K. I. Hardcastle, *Cryst. Growth Des.* **2011**, *11*, 843–850.
[36] J. Amato, T. Mashima, Y. O. Kamatari, K. Kuwata, E. Novellino, A. Randazzo, C. Giancola, M. Katahira, B. Pagano, *Nucleic Acid Ther.* **2020**, *30*, 414–421.
[37] H. Cantor, C. R. Warshaw, M. M. Shapiro, *Biopolymers* **1970**, *9*, 1059–1077.

Manuscript received: June 15, 2022
Revised manuscript received: July 28, 2022
Accepted manuscript online: August 8, 2022